2023 IEEE 9th International Workshop on Computational Advances in Multi-Sensor Adaptive Processing (CAMSAP) | 979-8-3503-4452-3/23/$31.00 ©2023 IEEE | DOI: 10.1109/CAMSAP58249.2023.10403499

Wavefront Engineering With Reconfigurable Intelligent Surfaces for Improved Sensing Capabilities in The THz Band

Arjun Singh[1], Priyansghu Sen[1], and Josep Miquel Jornet[2]
[1] Department of Engineering, SUNY Polytechnic Institute, Utica, NY
[2] Department of Electrical and Computer Engineering, Northeastern University, Boston, MA

Abstract

The terahertz (THz) band offers the advantages of massive available bandwidth and small signal wavelengths with revolutionary potential in both communication and sensing applications. However, the increased noise power from the larger bandwidth, as well as the increased path losses due to smaller wavelengths severely restrict the signal-to-noise ratio (SNR). In this light, reconfigurable intelligent surfaces (RISs) have been proposed as breakthrough devices that can be readily scaled up to create high-gain aperture systems, which are likely to have near-field applications. Here, wavefronts specifically engineered within the near field provide opportunities for improved sensing capabilities. Specifically, in this paper, we highlight how the greater depth of focus through Bessel beams can be utilized to improve the resolution capability of THz-band sensing. We numerically derive and show that Bessel beams can help improve target classification due to increased SNR in detection and increase resolution through increased bandwidth exploitation as well.

I. Introduction

Wireless sensing has been a feature of the wireless landscape for several years. In recent years, the feasibility of joint communications and sensing (JCS), and the need to provide very accurate channel sensing conditions within high-speed wireless links have only increased the demand for improvements in sensing technologies, both in terms of accuracy as well as reliability [1]–[3]. In this context, the Terahertz (THz, 0.3 – 10 THz) band has received significant attention, as the small wavelength of THz signals combined with the very wide bandwidth available at these frequencies can provide unprecedented sensing opportunities [3], [4].

Nonetheless, these opportunities at the THz band come at the cost of a high spreading/path loss, which can severely reduce the signal-to-noise ratio (SNR) and hence the applicable distance over which sensing can be confidently utilized. With the limitation of power output from on-chip power sources [5], [6], another method to boost the power is to direct it more effectively in the desired direction. For this, very large antenna arrays (VLAAs) can be utilized [7]. The gain of such a device depends on its dimensions, a sizeable THz VLAA, for example, a 10 cm array (similar to a mobile phone), can require several thousands of elements that cannot be easily integrated due to power losses, feeding issues, and thermal heat sinks [8]. Here, reconfigurable intelligent surfaces (RISs) provide a scalable alternative [8], [9] without the same feeding issue. RISs can be utilized both in the form of transmitting metasurfaces, helping to provide beamforming gain as the signal passes through them, or in the form of intelligent reflecting surfaces (IRSs), similar to reflectarrays, providing beamforming gain in reflection [8], [10].

However, it is relevant to note that the far-field distance of a radiating structure, or the region where conventional assumptions of beamforming are applicable, depends on the antenna size as $2D^2/\lambda$, where D is the largest antenna dimension [7]. Thus, although the physical size may be small, such as a few cm, the very small wavelengths of THz frequencies can result in many of these RISs having very large electrical apertures. The near-field of a THz-frequency sensing system is thus important and traditional beam management strategies, which imply a plane wave assumption with a uniform phase and where the spreading effect results in a Gaussian intensity [7], including those proposed for THz systems, can be inaccurate [11].

The inefficacy of conventional beamforming strategies requires a revisiting of the wave propagation phenomenon in near-field communication systems, which can be leveraged to, among others, provide a greater depth of focusing beam with higher SNR. Instead of exploring beamfocusing [11], which is the near-field counterpart of beamforming under the conventionally assumed spherical wave model, we derive the first principles of Bessel beams for sensing with RISs at THz frequencies and show significant opportunities in improved performance metrics, such as SNR, resolution, and bandwidth. The rest of the paper is organized as follows. In Sec. II, we revisit some wave propagation models for the near-field, and describe our system model and methodology in beam design. In Sec. III, we verify the potentially superior performance of Bessel beams in a near-field setup through numerical analyses and conclude our paper in Sec. IV.

II. Design Considerations

In this section, we first provide a brief summary of the different beam configurations that are discussed in the design

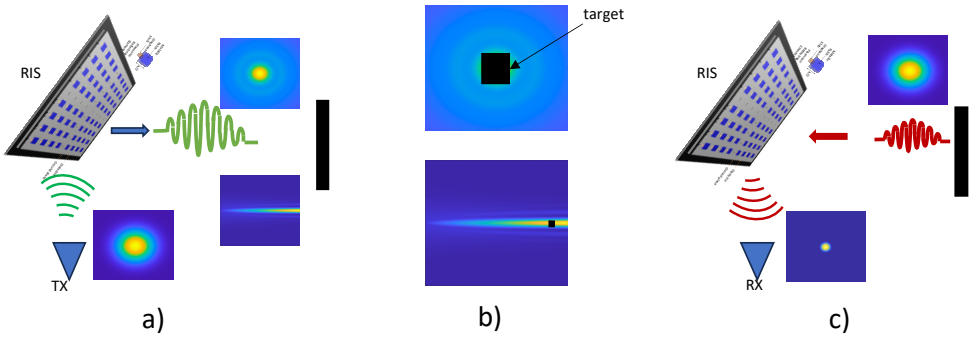

Fig. 1: A radar system utilizing wavefront engineering: a) The RIS converts an incident Gaussian beam into a Bessel beam; b) The non-diffracting Bessel beam interacts with the target, which blocks the central spot size with the top and bottom profiles showing the cross-sectional and transverse cuts; c) the reflected central spot size is received back at the RIS with a Gaussian intensity.

consideration. Next, we explain our system model and finally explain the design of the improved beam-shaping strategy under different possible configurations.

A. Wave Propagation in the Near Field

a) Beamfocusing and beamforming:

Beamfocusing and beamforming are two interrelated wave types that follow the spherical wave model. The transmitting array is configured with a quadratic phase profile to focus the signal at a particular focal point, wherein the wavefront converges to a singularity [11]. Beam intensity is maximum at this focal point, and the Abbe limit, which dictates the resolution capability of the array, gives the resultant beam spot size. Notably, if the focusing spot is instead redesigned to be at infinity, the resultant beam is then formed along a direction, giving the name of beamforming. The quadratic phase becomes a constant, uniform phase and the wavefront, or the imaginary line which connects all the points of a wave with the same phase, becomes planar. Beyond the far-field distance of $2D^2/\lambda$, the difference in the phase resulting from beamforming compared to beamfocusing is limited, at maximum, to $\pi/8$ [7]. Beamforming results in a beam that diverges in the far field due to limited aperture size. For an array in the x-y plane centered at $(0,0)$, the phase profile $C(\Phi)$ across the x-y plane that is required to focus the beam with wavevector k_0 at a point F away from the array is shown in (1) [12]:

$$C(\Phi) = k_0(\sqrt{F^2 + (x^2 + y^2)} - F). \tag{1}$$

As is evident, if F is replaced with infinity for beamforming, the phase becomes uniform [12]. In such a case, the beam is represented by a Gaussian intensity and is analogous to traditional beamforming. In the near-field, the Gaussian beam must be evaluated through diffraction optics [13]–[15], in which the beam waist is assumed to be the entire diameter of the array. We discuss this further in Sec. II-C.

b) Bessel beams:

In [16], solutions to wave propagation are provided by a wave profile with an intensity independent from the distance of propagation. In other words, such a wave is non-diffracting. The intensity of this beam is provided by a Bessel function, hence giving the name. In practice, this beam can be realized by a conical wave profile, and for a given beam to be generated by an array in the x-y plane centered at $(0,0)$, the phase profile $C(\Phi)$ that creates such a conical wave is [12]:

$$C(\Phi) = k_0\sqrt{x^2 + y^2}sin(\theta), \tag{2}$$

where θ describes the angle of the realized cone. The wave has two components, the transverse wavevector k_z for the planar propagation, and the radial wavevector k_r which governs how much the beam is focused, with $k_0 = \sqrt{k_z^2 + k_r^2}$. We discuss the specifics in Sec. II-C.

The simplest, or zero-order, Bessel beam profile has a central bright spot along the cone axis, with multiple concentric rings around it, which are interference patterns created from the interference of plane waves from the opposite sides of this central axis. Bessel beams are exact solutions to Maxwell's equations with a constant beam intensity. For a finite aperture and power, the propagation distance over which a practical Bessel beam retains its properties is limited, and governed by the relation between k_z and k_r. Bessel beams propagate in the near field, a feature absent in both beamforming and beamfocusing. Further, the intensity and the distance of propagation are all customizable, as we explain in Sec. II-C. Observing (2), we also see that even when the frequency changes, the resultant beam is still directed in the same direction, albeit for a different cone angle, which thus changes only the distance of propagation but not beam direction, making Bessel beams suitable to broadband systems.

B. System Model

We consider a radar system where the radar resolution τ is related to its bandwidth B by [17]:

$$\tau = \frac{c}{2B}, \tag{3}$$

where c is the speed of the signal. The transceiver can both transmit and receive the radar signal and leverages an RIS. The side length of the RIS is considered to be of size D

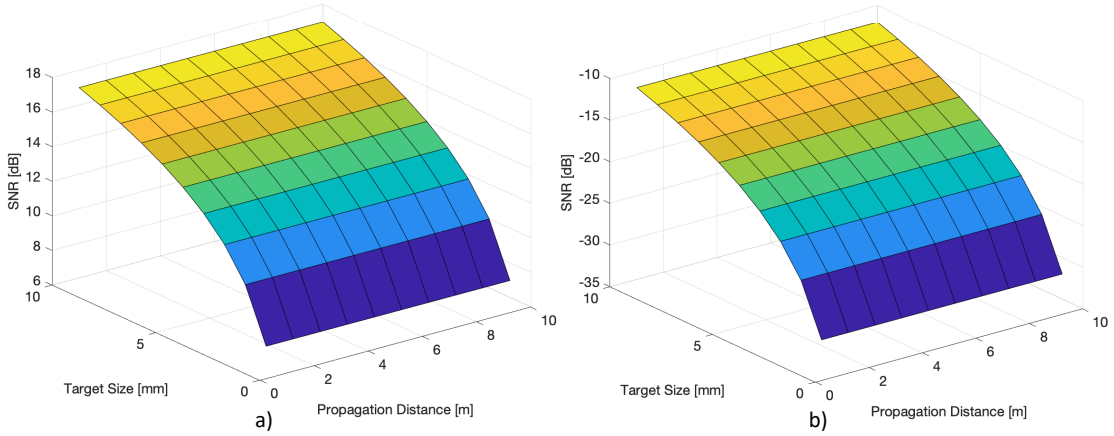

Fig. 2: SNR of a) Bessel and b) Gaussian beams under the specified conditions. The Bessel beam is updated to have a central spot size that matches the target size, which isn't possible with a Gaussian beam. The maximum distance is limited to the distance over which the Bessel beam is defined.

and it is assumed that there is no phase mismatch between RIS and transceiver. Thus, the RIS and the transceiver can interact with coherent signal reception and transmission. The RIS can then be utilized in the following manner – a) in transmission, the RIS is utilized to capture the Gaussian wave from a transmitter, and convert it into the desired wavefront (a Bessel beam), which is directed in the direction of the target; b) in receiving, the RIS receives a Gaussian reflection from the target end which is redirected towards the receiver.

As our work is aimed at first principles, we presently assume that the RIS is placed broadside from the target. Then, the phase profile on the RIS is given by the Huygens Fresnel wave propagation principle [18], wherein the complex amplitude $A(x, y, z)$ of the EM wave at any point from a given field distribution $A(\xi, \eta, 0)$ of any aperture situated at (ξ, η) orthogonal to the wave propagation direction z is given by:

$$A(x, y, z) = \frac{1}{j\lambda} \iint_S A(\xi, \eta, 0) \frac{\exp(-jkr_1)(1 + cos\psi)}{2r_1} \, d\xi \, d\eta. \tag{4}$$

Here, r_1 specifies the position vector of the point (x, y, z) while $cos\psi$ specifies the orientation from the z-axis. The complex field $A(\xi, \eta, 0)$ is given as $\S \exp(j\phi)$, where $\S$ is the magnitude and ϕ is the phase. When such a wave is incident on the RIS, it is within this phase ϕ that the phase transformation matrix from the elements of the RIS manifests in generating the resultant reflected complex field. Thus, with the knowledge of the orientation between the transmitter and the RIS, the RIS elements can be pre-configured to first remove any phase deviations due to orientation, and then add the phase for either beamforming as per (1) or Bessel beam as per (2). Wave propagation has time-reversal symmetry; thus, the opposite holds true as well; if a beam is reflected towards the RIS, the reflected wave would be redirected and add up coherently at the receiver.

Here, we observe that while in transmission, the beam profile can be generated as desired, in reflection, the shape of the target would play a vital role in deciding this setup. While it may be possible to utilize data-set and machine learning algorithms to quickly classify the shape of the target, at present, we consider a plane object such that it will reflect in-phase components. Thus, the signal reflected back towards the radar in reception is given by a Gaussian intensity. The summary of the system model is seen in Fig. 1.

C. Design of Bessel Beam for Sensing in the Near-Field

The intensity of a Bessel beam in the x-y plane is represented by $J_0(k_r\sqrt{x^2 + y^2})$, where $J_0(.)$ is the zero-order Bessel function [16]. Thus, for a given size of RIS aperture D, the number of rings that exist within $\sqrt{x^2 + y^2} \leq R$ define the number of concentric rings N that exist within the Bessel beam. The fraction of power P_{cs} contained within central spot size of width a, are given by [19]:

$$P_{cs} = P_T \left(\frac{a}{2D}\right), \tag{5}$$

where P_T is the total power at the array. We can observe that if the central spot size is a, then the requirement of $J_0(k_r\sqrt{x^2 + y^2}) = 0$ (so that the bright intensity ends) demands that we have:

$$k_r = 4.81/a, \tag{6}$$

since the first zero of the zero-order Bessel function is given by 2.405 [20]. Following k_r, we can next derive k_z:

$$k_z = \sqrt{k_0^2 - k_r^2}, \tag{7}$$

thus giving the requirement of generating the Bessel beam. The maximum range over which the Bessel beam can then be generated is given by $Z_{max} = R(k_z/k_r)$ [19]. This can also be approximated, in terms of the central spot size a, as:

$$Z_{max} = \pi Da/\lambda, \tag{8}$$

and thus, as long as the distance of propagation is less than Z_{max}, it becomes possible to derive a Bessel beam that has the central spot size a exactly as the size of the target we wish

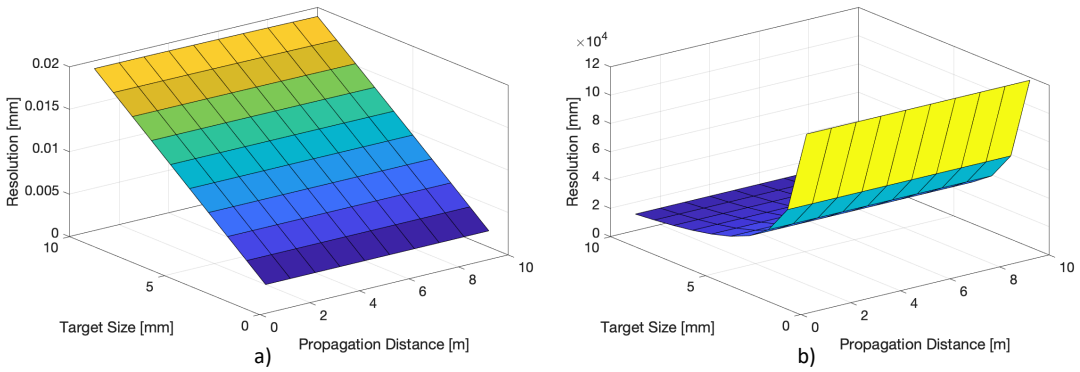

Fig. 3: Comparison of resolution capability with a reference bandwidth of 10 GHz: a) Bessel beams providing the same SNR as Gaussian and; b) Gaussian beam providing the same SNR as Bessel.

to detect, and thus maximize the power. The Bessel beam does not suffer from spreading, and thus the power doesn't reduce.

By contrast, a Gaussian beam which contains approximately 50% of its power in the central maximum and has a beam waist of w_0 will have the power distributed in a spot $w(z)$ at distance z, given by [15], [21]:

$$w(z) = \sqrt{1 + \left(\frac{z}{z_R}\right)^2}, \tag{9}$$

where z_R is the rayleigh range given by $z_R = \frac{\pi w_0^2}{\lambda_0}$, where λ_0 is the wavelength. Then, the fraction of power in the spot size a at distance z following [15] is:

$$P_{gaussian} = \frac{2P_T}{\pi} \frac{a}{w(z)^2}. \tag{10}$$

We thus observe that as the distance of propagation increases, the power within the target spot with a Gaussian beam will reduce, while it will remain the same for a Bessel beam.

III. Results

In this section, we utilize a numerical study utilizing MATLAB to analyze the performance of a radar system designed to operate in the near-field of a THz band, utilizing a design frequency of 1 THz, and a power of 1 mW, with a bandwidth of 10 GHz. The system is configured with an RIS that has a size of 10 $cm \times 10$ cm, which would have a nominal gain of 55 dBi.

Figure 2 shows the resultant SNR (Noise power spectral density, N_0, is considered $1 \times 10^{-16} W/Hz$ [22], [23]) as a function of both the size of the target as well as the propagation distance, in the case when the RIS generates either a Bessel beam or a Gaussian beam. When a Bessel beam is generated, the central spot size is set to match the size of the target, whereas in the case of the Gaussian beam, the beam waist is decided by the diameter of the RIS, or 10 cm. It is clearly seen that when the target size is increased, the amount of power that is reflected back increases in the case of both Bessel as well as Gaussian beams, with an increased SNR. However, in the case of Bessel beams, the ability to direct more energy into the specific beamspot that corresponds to the target size and is non-diffracting allows for a greatly increased depth of focus. In the case of Gaussian beams, the power is spread over a much larger area, and thus the target reflects back only a small amount of power, thus leading to inefficiency.

Figure 3(a) presents the resolution of the radar with the bandwidth available under the scheme of Bessel beams at the same SNR as was seen for a 10 GHz bandwidth Gaussian beam (Fig. 2(a)). Utilizing Bessel beams provides a greater signal power, thus freeing greater bandwidth without the limit of the noise factor. Consequently, the resolution possible can be further improved. Of course, a μm resolution as appears possible would require several THz of bandwidth and is thus purely theoretical, but the implication is obvious that bandwidth limitation due to low SNR is not a factor with Bessel beams in the near field. Equally interesting is the equivalent impact on the Gaussian configuration, when the noise power (due to bandwidth) is reduced enough for the same SNR as that available in the case of a Bessel configuration with the reference bandwidth of 10 GHz. This relation is presented in Fig. 3(b), and it is seen that the resolution has been truncated by almost three orders of magnitude due to the reduction in acceptable bandwidth to provide the same SNR.

IV. Conclusions

In this paper, we analyzed a near-field sensing setup for a radar-based target classification in the THz band, where we verified that the presume high gain of large RISs is in fact not valid for conventional beamforming, and thus pushes to evaluate other setups. Bessel beams, with highly favorable propagation conditions for both high frequency and high bandwidth systems, were shown to provide potentially superior performance in terms of both SNR as well as total bandwidth availability.

Our future work is aimed at studying the reflection of Bessel beams from irregular and imperfect obstacles.

References

[1] I. F. Akyildiz, C. Han, Z. Hu, S. Nie, and J. M. Jornet, "Terahertz band communication: An old problem revisited and research directions for the next decade," *IEEE Transactions on Communications*, vol. 70, no. 6, pp. 4250–4285, 2022.

[2] S. Aliaga, A. J. Alqaraghuli, A. Singh, and J. M. Jornet, "Enhancing joint communications and sensing for cubesat networks in the terahertz band through orbital angular momentum," in *2023 IEEE Aerospace Conference*. IEEE, 2023, pp. 1–14.

[3] H. Sarieddeen, N. Saeed, T. Y. Al-Naffouri, and M.-S. Alouini, "Next generation terahertz communications: A rendezvous of sensing, imaging, and localization," *IEEE Communications Magazine*, vol. 58, no. 5, pp. 69–75, 2020.

[4] I. F. Akyildiz, J. M. Jornet, and C. Han, "Terahertz band: Next frontier for wireless communications," *Physical Communication*, vol. 12, pp. 16–32, 2014.

[5] J. V. Siles, K. B. Cooper, C. Lee, R. H. Lin, G. Chattopadhyay, and I. Mehdi, "A new generation of room-temperature frequency-multiplied sources with up to 10× higher output power in the 160-ghz–1.6-thz range," *IEEE Transactions on Terahertz Science and Technology*, vol. 8, no. 6, pp. 596–604, 2018.

[6] K. Sengupta, T. Nagatsuma, and D. M. Mittleman, "Terahertz integrated electronic and hybrid electronic–photonic systems," *Nature Electronics*, vol. 1, no. 12, p. 622, 2018.

[7] C. A. Balanis, *Antenna theory: analysis and design*. John Wiley & Sons, 2016.

[8] C. Liaskos, S. Nie, A. Tsioliaridou, A. Pitsillides, S. Ioannidis, and I. Akyildiz, "A novel communication paradigm for high capacity and security via programmable indoor wireless environments in next generation wireless systems," *Ad Hoc Networks*, vol. 87, pp. 1–16, 2019.

[9] M. Di Renzo, M. Debbah, D.-T. Phan-Huy, A. Zappone, M.-S. Alouini, C. Yuen, V. Sciancalepore, G. C. Alexandropoulos, J. Hoydis, H. Gacanin *et al.*, "Smart radio environments empowered by reconfigurable ai meta-surfaces: An idea whose time has come," *EURASIP Journal on Wireless Communications and Networking*, vol. 2019, no. 1, pp. 1–20, 2019.

[10] A. Singh, V. Petrov, H. Guerboukha, I. V. A. K. Reddy, E. W. Knightly, D. M. Mittleman, and J. M. Jornet, "Wavefront engineering: Realizing efficient terahertz band communications in 6G and beyond," *to appear in the IEEE Wireless Communications Magazine*, 2023.

[11] M. Cui, Z. Wu, Y. Lu, X. Wei, and L. Dai, "Near-Field MIMO communications for 6G: Fundamentals, challenges, potentials, and future directions," *IEEE Communications Magazine*, vol. 61, no. 1, pp. 40–46, January 2023.

[12] D. Headland, Y. Monnai, D. Abbott, C. Fumeaux, and W. Withayachumnankul, "Tutorial: Terahertz beamforming, from concepts to realizations," *Apl Photonics*, vol. 3, no. 5, p. 051101, 2018.

[13] J. Alda, "Laser and gaussian beam propagation and transformation," *Encyclopedia of optical engineering*, vol. 999, pp. 1013–1013, 2003.

[14] R. Paschotta, "Encyclopedia of laser physics and technology," *(No Title)*, 2008.

[15] S. A. Self, "Focusing of spherical gaussian beams," *Applied optics*, vol. 22, no. 5, pp. 658–661, 1983.

[16] J. Durnin, "Exact solutions for nondiffracting beams. I. the scalar theory," *JOSA A*, vol. 4, no. 4, pp. 651–654, 1987.

[17] D. R. Wehner, "High resolution radar," *Norwood*, 1987.

[18] F. Depasse, M. Paesler, D. Courjon, and J. Vigoureux, "Huygens–fresnel principle in the near field," *Optics letters*, vol. 20, no. 3, pp. 234–236, 1995.

[19] J. Durnin, J. Miceli, and J. H. Eberly, "Comparison of bessel and gaussian beams," *Optics letters*, vol. 13, no. 2, pp. 79–80, 1988.

[20] A. Matijošius, V. Jarutis, and A. Piskarskas, "Generation and control of the spiraling zero-order bessel beam," *Optics Express*, vol. 18, no. 9, pp. 8767–8771, 2010.

[21] D. C. O'shea and D. C. C'Shea, *Elements of modern optical design*. Wiley New York, 1985, vol. 2.

[22] P. Sen, D. A. Pados, S. N. Batalama, E. Einarsson, J. P. Bird, and J. M. Jornet, "The teranova platform: An integrated testbed for ultra-broadband wireless communications at true terahertz frequencies," *Computer Networks*, vol. 179, p. 107370, 2020.

[23] P. Sen, V. Ariyarathna, A. Madanayake, and J. M. Jornet, "A versatile experimental testbed for ultrabroadband communication networks above 100 ghz," *Computer Networks*, vol. 193, p. 108092, 2021.